



OPEN

SUBJECT AREAS:

INFORMATION STORAGE
MAGNETIC PROPERTIES AND
MATERIALSReceived
20 March 2014Accepted
14 July 2014Published
31 July 2014Correspondence and
requests for materials
should be addressed to
J.W.C. (jwcai@iphy.
ac.cn)

Thermally robust Mo/CoFeB/MgO trilayers with strong perpendicular magnetic anisotropy

T. Liu¹, Y. Zhang¹, J. W. Cai¹ & H. Y. Pan²

¹Beijing National Laboratory for Condensed Matter Physics, Institute of Physics, Chinese Academy of Sciences, Beijing 100190, China, ²Key Laboratory for the Physics and Chemistry of Nanodevices, Department of Electronics, School of Electronics Engineering and Computer Science, Peking University, Beijing, 100871, China.

The recent discovery of perpendicular magnetic anisotropy (PMA) at the CoFeB/MgO interface has accelerated the development of next generation high-density non-volatile memories by utilizing perpendicular magnetic tunnel junctions (*p*-MTJs). However, the insufficient interfacial PMA in the typical Ta/CoFeB/MgO system will not only complicate the *p*-MTJ optimization, but also limit the device density scalability. Moreover, the rapid decreases of PMA in Ta/CoFeB/MgO films with annealing temperature higher than 300 °C will make the compatibility with CMOS integrated circuits a big problem. By replacing the Ta buffer layer with a thin Mo film, we have increased the PMA in the Ta/CoFeB/MgO structure by 20%. More importantly, the thermal stability of the perpendicularly magnetized (001)CoFeB/MgO films is greatly increased from 300 °C to 425 °C, making the Mo/CoFeB/MgO films attractive for a practical *p*-MTJ application.

Magnetic tunnel junctions (MTJs) with ferromagnetic electrodes possessing perpendicular magnetic anisotropy (PMA) have the potential for realizing high-density magnetoresistance random access memories (MRAMs)^{1,2}. Such MTJs combine several important advantages over the MTJs with in-plane anisotropy, such as higher energy barrier against thermal agitation at reduced dimensions, smaller critical current density and faster reversal speed for current induced magnetization switching (CIMS)^{3–5}. However, all the conventional PMA materials, including rare-earth/transition-metal alloys^{6,7}, L1₀-ordered (Co, Fe)-(Pt, Pd) alloys^{8,9}, and Co/(Pd, Pt, Ni) multilayers^{10,11}, suffer from either insufficient chemical/thermal stability or difficulties in integrating them into MTJs. In fact, the perpendicular MTJs (*p*-MTJs) based on these materials exhibit a relatively low magnetoresistance ratio and a high critical current needed for CIMS due to their low spin polarization and large Gilbert damping constant^{6–11}. The discovery of appreciable interfacial PMA in the Ta/CoFeB/MgO films together with the demonstration of high performance *p*-MTJs by utilizing this well developed material system is a real breakthrough². Further study showed that an electric field can be used to assist magnetization switching with the electric current density reduced by two orders in the perpendicular CoFeB/MgO MTJs¹². These findings represent significant steps towards the next generation spintronic devices. However, the interfacial PMA in the Ta/CoFeB/MgO system is insufficient for practical applications to some extent. It will not only limit the device density scalability, but also complicate *p*-MTJ optimization considering the ultrathin CoFeB layer with a very narrow tunable thickness range. Moreover, the rapid decrease of PMA in Ta/CoFeB/MgO films with the annealing temperature higher than 300 °C significantly degrades the performance of the *p*-MTJs^{13–16}. Since MRAMs with multi-level interconnects require a processing temperature of 350 °C or higher^{17,18}, it is urgently demanded to improve the thermal stability of the perpendicular CoFeB/MgO films. By replacing the Ta buffer with a Hf layer, we were able to raise the PMA of CoFeB/MgO films by 30% but without improvement in its thermal stability¹⁹. In this paper, we have explored the effect of Mo buffer on the magnetic properties of CoFeB/MgO films, and found that the Mo/CoFeB/MgO films can endure thermal annealing at temperatures of up to 425 °C along with appreciable enhancement in the PMA.

Results

Films of Ta(5)/Co₄₀Fe₄₀B₂₀(0.8–1.8)/MgO(2)/Ta(5) and Mo(5)/Co₄₀Fe₄₀B₂₀(0.8–1.8)/MgO(2)/Mo(5) (in nm) annealed at a relatively low temperature of 300 °C were first characterized magnetically. Figures 1(a) and (b) show the representative M–H curves of the Ta/CoFeB/MgO films with the external field perpendicular and parallel to

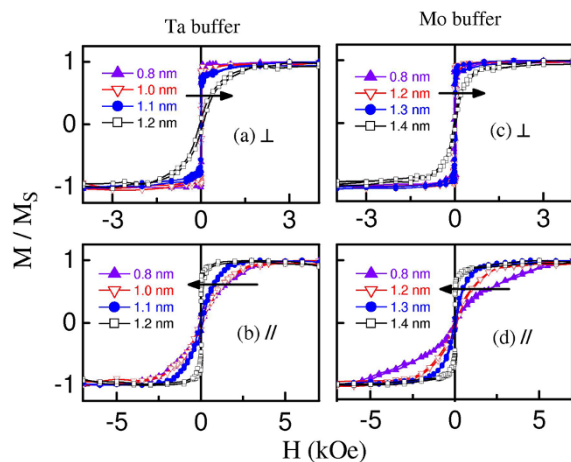


Figure 1 | M-H curves of representative samples annealed at 300 °C. (left panel) Ta(5)/Co₄₀Fe₄₀B₂₀(*t*_{CoFeB})/MgO(2)/Ta(5) and (right panel) Mo(5)/Co₄₀Fe₄₀B₂₀(*t*_{CoFeB})/MgO(2)/Mo(5) (in nm) with external field perpendicular (a), (c), and parallel (b), (d) to the film plane. The numbers in the figures correspond to the CoFeB layer thickness.

the film, respectively. PMA is only observed for *t*_{CoFeB} ≤ 1.1 nm, for thicker films the magnetic easy axis of the CoFeB layer is in the film plane, in agreement with previous work^{2,12}. For the Mo/CoFeB/MgO films prepared and annealed under the same conditions, the M-H curves in Fig. 1(c) and 1(d) reveal that perpendicular magnetization presents in the CoFeB layer with thickness up to 1.3 nm. It suggests that the Mo buffer is more beneficial to the PMA than Ta.

From the M-H curves of the 300 °C annealed samples, the effective perpendicular anisotropy (*K*_{eff}) and areal saturation magnetization (*m*) were determined. The inset of Fig. 2 shows the CoFeB thickness dependence of areal saturation magnetization for the Ta and Mo buffered CoFeB/MgO films. There is little difference between these two series samples. The linear fitting on *m* versus *t*_{CoFeB}, *m* = *M*_S(*t*_{CoFeB} - *t*_d), gives the CoFeB saturation magnetization (*M*_S) of about 1600 emu/cm³ without magnetic dead layer (*t*_d) formation for both Ta and Mo buffered films. The *M*_S value of the as-deposited films was measured to be about 1040 emu/cm³. The large increase in *M*_S upon annealing suggests the crystallization of CoFeB layers during the heat treatment. Figure 2 shows *t*_{CoFeB} dependences of the *K*_{eff}*t*_{CoFeB} product for Ta/CoFeB/MgO and Mo/CoFeB/MgO films annealed at 300 °C. By fitting the data through the equation,

$$K_{\text{eff}} = (K_V - 2\pi M_S^2) + K_S/t_{\text{CoFeB}},$$

the CoFeB volume anisotropy (*K*_V) is found to be negligible and the interfacial anisotropy (*K*_S) is about 1.7 erg/cm² and 2.05 erg/cm² for the Ta and Mo buffered samples, respectively. The interfacial PMA increases by 20%, leading to the perpendicularly magnetized Mo/CoFeB/MgO films with a thicker CoFeB layer as observed above. It should be pointed out that, the origin of the well-known PMA in Ta/CoFeB/MgO films is complex and still under debate^{19–23}. While the CoFeB/MgO interface has been widely demonstrated to present a large interfacial anisotropy, it is controversial whether the interface between Ta and CoFeB layers partially contributes to the PMA or not. From the different PMA results for CoFeB/MgO films grown on different buffer layers, it is believed that interfacial anisotropy is generated at the Ta/CoFeB interface^{21–23}. However, considering the fact that there is no PMA component found in the Ta/CoFeB/Ta films, it looks like the PMA in Ta/CoFeB/MgO films solely originated from the CoFeB/MgO interface¹⁹. The problem encountered for both hypotheses is similar, i.e. the structure/microstructure of the thin CoFeB layer as well as its interfaces might be altered for the CoFeB/MgO films grown on different buffers or the Ta/CoFeB films covered by different capping layers, especially considering the crys-

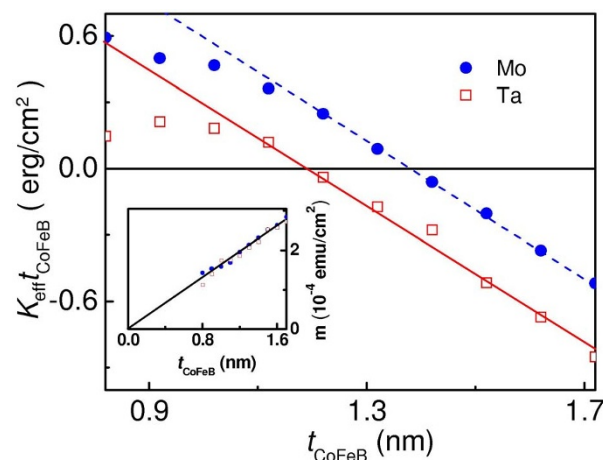


Figure 2 | Quantitative analysis of magnetic properties for samples annealed at 300 °C. Dependence of the product *K*_{eff}*t*_{CoFeB} on *t*_{CoFeB} for the films Ta(5)/Co₄₀Fe₄₀B₂₀(*t*_{CoFeB})/MgO(2)/Ta(5) and Mo(5)/Co₄₀Fe₄₀B₂₀(*t*_{CoFeB})/MgO(2)/Mo(5) (in nm) annealed at 300 °C. Inset: dependence of areal saturation magnetization on CoFeB layer thickness for the 300 °C annealed samples. The straight lines are the linear fitting results.

tallization and possible intermixing during the annealing process. In order to compare the effects of Mo and Ta with minimized structural factor, an additional series of films MgO(5)/CoFeB(0.5*t*)/X/CoFeB(0.5*t*)/MgO(5) (*t* = 1.1–4 nm; X = 0.2 nm Mo or none) were fabricated and annealed at 300 °C for two hours. Magnetic measurements show that the addition of a Mo submonolayer into the MgO/CoFeB/MgO structure increases the CoFeB/MgO interface anisotropy from 0.6 erg/cm² to 1.25 erg/cm², equal to that obtained in the same structure with 0.2 nm Ta addition¹⁹. This means that the dusting of Mo and Ta atoms induces similar interface anisotropy enhancement. Thus, there must be additional factors making *K*_S of the Mo/CoFeB/MgO films larger than that of Ta buffered samples. It was proposed that the buffer layer with a high negative formation enthalpy for its boride compounds may lead to better crystallization of the CoFeB/MgO interface and thus improving *K*_S^{24,25}. Clearly this is not the case here, because molybdenum borides were predicted to have much smaller enthalpies in comparison with tantalum borides²⁶. The stress effect of the Mo buffer, if any, is also eliminated by the fact of *K*_S enhancement in the Ta/ultra thin Mo/CoFeB/MgO films as shown later. The PMA of Ta/CoFeB/MgO films was found to exhibit the maximum value at the annealing temperature of 250 °C due to the Ta/CoFeB intermixing at higher temperatures^{16,27}. The little interdiffusion in Mo buffered CoFeB/MgO films, which will be proved below, likely contributes to the larger *K*_S in the Mo/CoFeB/MgO films annealed at 300 °C.

We then studied the magnetic properties of the perpendicularly magnetized CoFeB/MgO films with Ta and Mo buffers at different annealing temperatures. For the Ta/CoFeB/MgO films, annealing at temperatures above 300 °C leads to the collapse of the perpendicular magnetic anisotropy together with appreciable moment loss. Figure 3(a) and (b) show the M-H loops of the representative Ta/CoFeB/MgO films annealed at 325 °C. Note that, the film with *t*_{CoFeB} = 1.0 nm turns to exhibit in-plane anisotropy, whereas the sample with *t*_{CoFeB} = 0.8 nm even has zero remanence with rounded in-plane and perpendicular M-H curves coinciding with each other, resembling superparamagnetism. Meanwhile, both samples show the areal saturation magnetization reduced almost by half in comparison with the 300 °C annealed films [cf. inset of Fig. 2]. When the annealing temperature increases to 350 °C, the Ta/CoFeB/MgO films are further deteriorated. In addition to more moment loss, all films with *t*_{CoFeB} ≤ 1.1 nm present superparamagnetic-like M-H curves (not shown). These results are in agreement with those reported

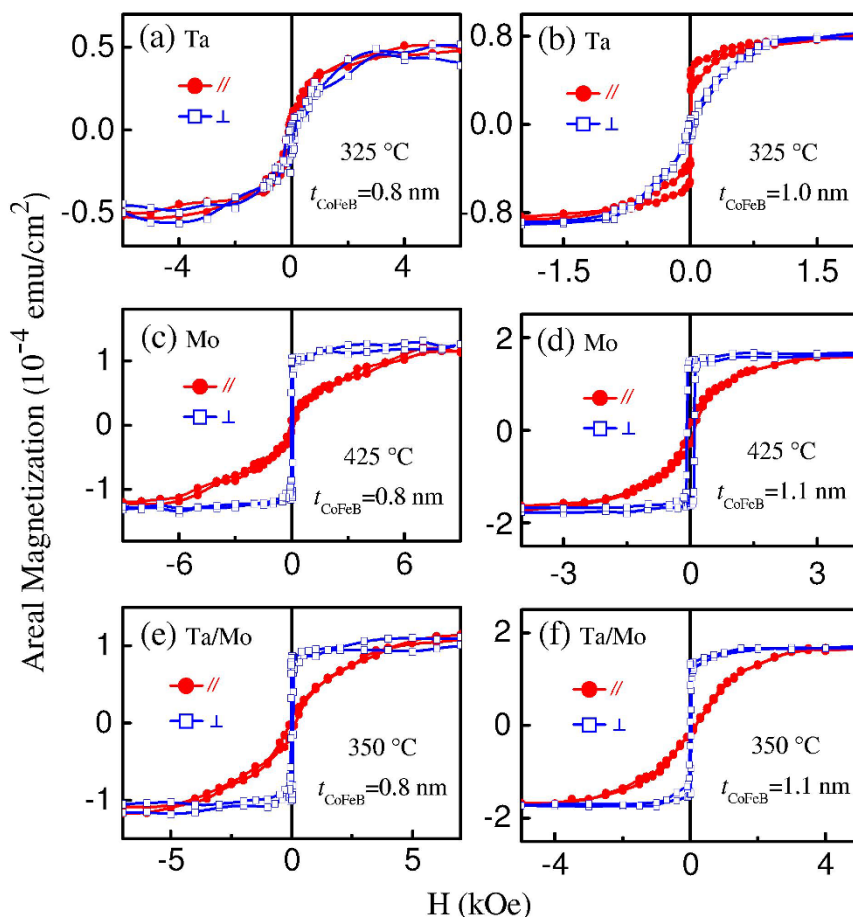


Figure 3 | M-H curves of representative samples annealed at elevated temperature. (a) (b) Ta(5)/Co₄₀Fe₄₀B₂₀(*t*_{CoFeB})/MgO(2)/Ta(5) after annealing at 325 °C; (c) (d) Mo(5)/Co₄₀Fe₄₀B₂₀(*t*_{CoFeB})/MgO(2)/Mo(5) after annealing at 425 °C; and (e) (f) Ta(5)/Mo(0.5)/Co₄₀Fe₄₀B₂₀(*t*_{CoFeB})/MgO(2)/Ta(5) (in nm) after annealing at 350 °C.

recently^{13,16,27}. Overall, the perpendicularly magnetized Ta/CoFeB/MgO films are rather unstable against annealing. It should be pointed out that, Ta interdiffusion has been demonstrated in magnetic multilayer films after heat treatment, which not only degrades MTJs, but also causes significant moment loss and PMA deterioration, especially for the perpendicularly magnetized Ta/CoFeB/MgO films with a very thin CoFeB layer^{27–30}.

For the Mo/CoFeB/MgO films, the large interfacial perpendicular magnetic anisotropy remains unchanged and all trilayers with $t_{\text{CoFeB}} \leq 1.2$ nm exhibit perpendicular magnetization after annealing at temperature (T_{an}) up to 425 °C. Figure 3(c) and (d) display M-H curves of the 425 °C annealed Mo/CoFeB/MgO films with $t_{\text{CoFeB}} = 0.8$ and 1.1 nm, respectively. A square perpendicular loop is evident with remanence ratio exceeding 0.9 for both samples. The effective perpendicular magnetic anisotropy field, estimated from the in-plane M-H curve, is about 6 kOe for $t_{\text{CoFeB}} = 0.8$ nm and 1.5 kOe for $t_{\text{CoFeB}} = 1.1$ nm, comparable to the values for the 300 °C annealed samples. Clearly the strong PMA for the trilayers with a thin CoFeB layer is maintained after the extremely high temperature annealing. It should be mentioned that there is no magnetic dead layer formation with the magnetization even slightly larger than that of the 300 °C annealed films, which will be detailed later. Parenthetically, since the shape anisotropy increases with the increase of the magnetization, the Mo/CoFeB/MgO film with $t_{\text{CoFeB}} = 1.3$ nm after annealing at 425 °C no longer shows perpendicular magnetization. In summary, by simply replacing the typical Ta buffer with a Mo layer, a thermally robust perpendicularly magnetized CoFeB/MgO system is realized. This result also suggests that there is little Mo

interdiffusion during the high temperature annealing, even for the case of the extremely thin CoFeB layer. We have further studied the films of Ta(5)/Mo(0.5)/Co₄₀Fe₄₀B₂₀(0.8–1.8)/MgO(2)/Ta(5) (in nm) annealed at different temperatures. In contrast to the Ta/CoFeB/MgO film, the Ta/Mo(0.5)/CoFeB/MgO film with $0.8 \text{ nm} \leq t_{\text{CoFeB}} \leq 1.1$ nm presents well defined PMA at $T_{\text{an}} \leq 350$ °C, indicative of the significantly improved thermal stability. Figure 3(e) and (f) show M-H curves of the 350 °C annealed Ta/Mo(0.5)/CoFeB/MgO films with $t_{\text{CoFeB}} = 0.8$ and 1.1 nm, respectively. The samples have large effective perpendicular magnetic anisotropy field along with the unreduced magnetization. It is likely that the serious diffusion of Ta into the thin CoFeB layer in the Ta/CoFeB/MgO films at $T_{\text{an}} = 350$ °C is effectively hampered by the ultrathin Mo insertion layer, showing the crucial role of Mo as a diffusion barrier in magnetic multilayers.

Based on the M-H curves of various CoFeB thicknesses, the interface anisotropy (K_s), the CoFeB saturation magnetization (M_s), and the nominal magnetic dead layer thickness (t_d) were determined for both Ta/CoFeB/MgO and Mo/CoFeB/MgO films annealed at temperatures between 300–450 °C. The results are summarized in Fig. 4. Note that for the Ta/CoFeB/MgO films, K_s sharply decreases from 1.7 to 1.2 erg/cm² as T_{an} increases from 300 to 325 °C, and further falls to 0.9 erg/cm² at $T_{\text{an}} = 350$ °C; Meanwhile, a magnetic dead layer that is equivalent to the observed large moment loss is given as $t_d = 0.45$ nm at $T_{\text{an}} = 325$ °C and $t_d = 0.55$ nm at $T_{\text{an}} = 350$ °C. With the dead layer part subtracted, the M_s of the CoFeB layers changes minimally in this annealing temperature range. All these parameters indicate the serious deterioration of the CoFeB layer

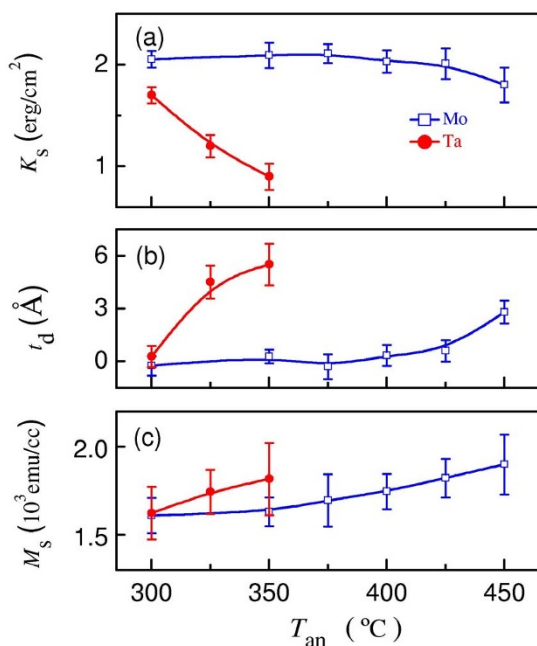


Figure 4 | Magnetic parameters of the Ta/CoFeB/MgO and Mo/CoFeB/MgO films annealed at different temperatures. The annealing temperature T_{an} dependences of (a) interfacial anisotropy K_s , (b) nominal magnetic dead layer thickness t_d , and (c) CoFeB saturation magnetization M_s for films Ta(5)/Co₄₀Fe₄₀B₂₀(t_{CoFeB})/MgO(2)/Ta(5), Mo(5)/Co₄₀Fe₄₀B₂₀(t_{CoFeB})/MgO(2)/Mo(5) (in nm).

due to the interdiffusion at $T_{an} > 300^\circ\text{C}$. For the Mo/CoFeB/MgO films, the large K_s is maintained within 2.05 ± 0.07 erg/cm² at $300^\circ\text{C} \leq T_{an} \leq 425^\circ\text{C}$, and there is almost no magnetic dead layer formation. The apparent K_s decrease and appreciable magnetic dead layer formation are observed at the elevated annealing temperature of 450°C . The M_s of Mo/CoFeB/MgO films slightly increases till $T_{an} = 375^\circ\text{C}$, then it rises at a faster rate. Such increase in M_s should be caused by CoFeB crystallization improvement. In short, the Mo/CoFeB/MgO films with larger PMA are thermally stable up to 425°C . Parenthetically, the K_s of the 300°C annealed Ta/Mo(0.5)/CoFeB/MgO films was determined to be about 1.85 erg/cm², slightly larger than that for Ta/CoFeB/MgO. This K_s value is unchanged at $T_{an} = 350^\circ\text{C}$, but sharply decreases to 1.4 erg/cm² at $T_{an} = 375^\circ\text{C}$, accompanied with a dead layer increasing from 1 Å to 4 Å. This result indicates that the interfacial ultrathin Mo between Ta and CoFeB layers considerably improves PMA and the thermal stability due to the suppressed Ta interdiffusion.

Besides the thorough investigation of the CoFeB/MgO films grown on a Ta or Mo buffer layer, the films with the inverted structure, namely MgO(5)/Co₄₀Fe₄₀B₂₀(0.8–1.8)/Ta(5) or Mo(5) (in nm), were also examined. After annealing at 300°C , the Ta and Mo capped MgO/CoFeB films show perpendicular magnetization with the same upper limit thickness of 1.5 nm for the CoFeB layer in both sets samples. However, the MgO/CoFeB/Ta films have a nominal dead layer thickness of about 0.5 nm whereas the MgO/CoFeB/Mo films only about 0.25 nm. The dead layer formation in MgO/CoFeB/Ta films was reported previously². Clearly, this dead layer thickness is reduced in the MgO/CoFeB/Mo films. Moreover, the magnitude of K_s is about 1.6 erg/cm² for the Ta capped films, and 1.9 erg/cm² for the Mo capped samples. Both values are slightly lower than the results obtained in the Ta and Mo buffered samples, showing the effect of the stacking sequence. Most importantly, serious magnetic deterioration occurs in MgO/CoFeB/Ta at $T_{an} = 325^\circ\text{C}$, but there is neither PMA worsening nor further moment loss in MgO/CoFeB/Mo when T_{an} is elevated up to 425°C . These results indicate that the

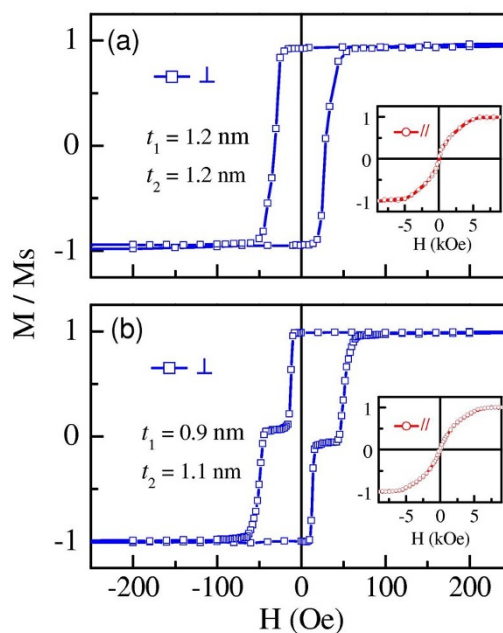


Figure 5 | M-H curves of the multilayered Mo/CoFeB/MgO/CoFeB/Mo films annealed at 400°C . (a) Mo(5)/Co₄₀Fe₄₀B₂₀(1.2)/MgO(2)/Co₄₀Fe₄₀B₂₀(1.2)/Mo(5), and (b) Mo(5)/Co₄₀Fe₄₀B₂₀(0.9)/MgO(2)/Co₄₀Fe₄₀B₂₀(1.1)/Mo(5) (in nm).

MgO/CoFeB films covered by Mo also present larger PMA and significantly improved thermal stability.

Finally, in order to evaluate the suitability of the Mo-based CoFeB/MgO films for practical *p*-MTJs application, the multilayer films of Mo(5)/Co₄₀Fe₄₀B₂₀(0.8–1.2)/MgO(2)/Co₄₀Fe₄₀B₂₀(0.8–1.2)/Mo(5) (in nm) annealed at 400°C were characterized magnetically and structurally. First of all, strong PMA presents in all these multilayer films after high temperature annealing. Figure 5 shows M-H curves of two representative samples, Mo/CoFeB(1.2)/MgO/CoFeB(1.2)/Mo and Mo/CoFeB(0.9)/MgO/CoFeB(1.1)/Mo. Note that, perpendicular magnetization is evident even for the multilayer with the top and bottom CoFeB layers as thick as 1.2 nm. Because of the small switching field difference, the top and bottom CoFeB layers with the same thickness simultaneously switch their perpendicular magnetization via the domain nucleation mechanism. It was previously shown that, independent magnetization switches were achieved in sub-micrometer size patterned MTJs even for such a symmetric stack due to the subtle difference in individual layer microstructures and dimensions². By adjusting the CoFeB thickness, as shown in Fig. 5(b), appreciable different switching fields for the top and bottom CoFeB layers can also be readily achieved in the asymmetric multilayer stack. In short, magnetically the multilayer structure Mo/CoFeB/MgO/CoFeB/Mo is suitable for *p*-MTJs with strong thermal stability.

Figure 6(a) shows the cross-section high-resolution transmission electron microscopy (HRTEM) image of the 400°C annealed Mo(5)/CoFeB(1.2)/MgO(2)/CoFeB(1.2)/Mo(5) (in nm) film. The stacking structure of different continuous layers is clear. The fast Fourier transforms (FFT) from the square area “b” across the interface is shown in Fig. 6(b), where the bcc [110] zone axis of CoFeB and the fcc [100] zone axis of MgO can be identified as the spots marked out by circles and triangles, respectively. The (002) diffraction spots of bcc CoFeB and fcc MgO are indexed in their corresponding diffraction pattern, which is along the layer stacking direction. Figure 6(c) presents the FFT diffraction spots from the “c” region of Mo layer. This pattern corresponds well with bcc [001] zone axis with (110) indexed. The planar selected area electron diffraction pattern from the same film is displayed in Fig. 6(d). The polycrystalline diffraction rings match the different layer orientation perpendicular to the film. These

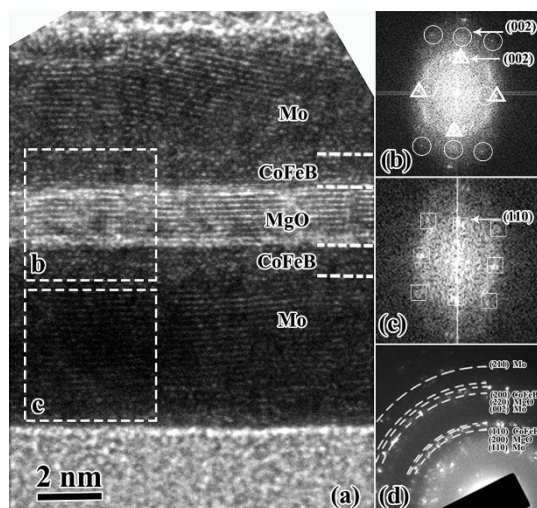


Figure 6 | Structural characterization of the multilayer film Mo(5)/Co₄₀Fe₄₀B₂₀ (1.2)/MgO(2)/Co₄₀Fe₄₀B₂₀(1.2)/Mo(5) (in nm) annealed at 400 °C. (a) The cross-section HRTEM images of the Mo/CoFeB/MgO/CoFeB/Mo film annealed at 400 °C; (b–c) FFT diffraction patterns from square interface region “b” and Mo region “c”, respectively; (d) Selected area electron diffraction pattern of the planar multilayer film.

results demonstrate that, while the Mo buffer of bcc structure has a (110) texture, the CoFeB and MgO layers exhibit bcc(001) and fcc(001) texture perpendicular to the film, respectively. The crystallization of the CoFeB layers is dominated by the template effect of MgO during annealing. The formation of (001) texture in CoFeB and MgO layers is essential to giant tunneling magnetoresistance in MgO-based MTJs. The present Mo/CoFeB/MgO/CoFeB/Mo structure fulfills the requirements of practical *p*-MTJ application. The microfabrication of *p*-MTJ devices based on this structure and evaluation of the TMR are beyond the scope of the present paper, we expect that this interesting issue will be investigated in the spintronic community.

Discussion

It is known that both Tantalum and Molybdenum are highly refractory materials. Some characteristics about these two materials have to be considered to account for the significant improvement of perpendicular magnetic properties against thermal annealing in the Mo/CoFeB/MgO films. First, the Tantalum oxide with a very high negative formation enthalpy (−2046 kJ/mol) is thermodynamically more stable than MgO (−602 kJ/mol)³¹, this may reinforce the Ta diffusion towards the CoFeB/MgO interface during annealing. In contrast, with the formation enthalpies of Molybdenum oxides (−589 kJ/mol for MoO₂ and −745 kJ/mol for MoO₃) comparable to that of MgO, the Mo atoms should be hardly affected by the presence of MgO layer nearby. Secondly, the thin Ta film sputtered on a thermally oxidized Si substrate is amorphous, whereas the sputtered Mo film has a crystalline structure. Since the metastable amorphous structure has a higher energy, the out-diffusion of the amorphous atoms can be accelerated during annealing as observed by Yamanouchi et al.²⁷ From the structural point of view, the interdiffusion of Ta in the Ta/CoFeB/MgO samples can be also intensified, whereas the Mo atoms stay in the stable state.

In conclusion, it is the superior thermal endurance of molybdenum that makes the perpendicularly magnetized Mo/CoFeB/MgO films highly stable. With enhanced perpendicular magnetic anisotropy and negligible detrimental intermixing after two hours annealing at temperatures of up to 425 °C, the Mo buffered (001)CoFeB/MgO films are very promising for practical perpendicular magnetic tunnel junction application.

Methods

Samples in this work mainly include three sets of CoFeB/MgO films with different buffer layers and one set of CoFeB/MgO/CoFeB multilayers, i.e.

- (1) Ta(5)/Co₄₀Fe₄₀B₂₀(0.8–1.8)/MgO(2)/Ta(5) and the inverted, MgO(5)/Co₄₀Fe₄₀B₂₀(0.8–1.8)/Ta(5),
- (2) Mo(5)/Co₄₀Fe₄₀B₂₀(0.8–1.8)/MgO(2)/Mo(5) and the inverted, MgO(5)/Co₄₀Fe₄₀B₂₀(0.8–1.8)/Mo(5),
- (3) Ta(5)/Mo(0.5)/Co₄₀Fe₄₀B₂₀(0.8–1.8)/MgO(2)/Ta(5),
- (4) Mo(5)/Co₄₀Fe₄₀B₂₀(0.8–1.2)/MgO(2)/Co₄₀Fe₄₀B₂₀(0.8–1.2)/Mo(5),

where the numbers in the brackets are the nominal thickness of the individual layers in nanometer (nm). All films were deposited on the thermally oxidized Si wafers at room temperature by magnetron sputtering. The base pressure of the sputtering system was lower than 4×10^{-5} Pa and working argon pressure was 0.5 Pa. The films of Mo, Ta and Co₄₀Fe₄₀B₂₀ were dc sputtered from the respective Mo, Ta and Co₄₀Fe₄₀B₂₀ alloy targets, whereas the MgO layer was deposited from a MgO target by rf sputtering. Up to 18 uniform films were prepared in a single deposition run. All samples were subsequently annealed at 300–450 °C for two hours in vacuum (3×10^{-5} Pa). Magnetic properties were studied using vibrating sample magnetometer (VSM). The microstructure characterization was performed on FEI Tecnai F30 scanning transmission electron microscopy (STEM). Cross-section TEM samples were prepared using a standard procedure consisting of gluing, wire saw cutting, mechanical polishing, dimpling, and ion milling. All presented results are obtained from room temperature measurements on the annealed samples unless otherwise specified.

1. Mangin, S. *et al.* Current-induced magnetization reversal in nanopillars with perpendicular anisotropy. *Nat. Mater.* **5**, 210–215 (2006).
2. Ikeda, S. *et al.* A perpendicular-anisotropy CoFeB–MgO magnetic tunnel junction. *Nat. Mater.* **9**, 721–724 (2010).
3. Slonczewski, J. C. Current-driven excitation of magnetic multilayers. *J. Magn. Magn. Mater.* **159**, L1–L7 (1996).
4. Sun, J. Z. Spin-current interaction with a monodomain magnetic body: A model study. *Phys. Rev. B* **62**, 570–578 (2000).
5. Worledge, D. C. *et al.* Spin torque switching of perpendicular Ta/CoFeB/MgO-based magnetic tunnel junctions. *Appl. Phys. Lett.* **98**, 022501 (2011).
6. Nishimura, N. *et al.* Magnetic tunnel junction device with perpendicular magnetization films for high-density magnetic random access memory. *J. Appl. Phys.* **91**, 5246–5249 (2002).
7. Ohmori, H., Hatori, T. & Nakagawa, S. Perpendicular magnetic tunnel junction with tunneling magnetoresistance ratio of 64% using MgO (100) barrier layer prepared at room temperature. *J. Appl. Phys.* **103**, 07A911 (2008).
8. Yoshikawa, M. *et al.* Tunnel magnetoresistance over 100% in MgO-based magnetic tunnel junction films with perpendicular magnetic L1₀-FePt electrodes. *IEEE Trans. Magn.* **44**, 2573–2576 (2008).
9. Kim, G. *et al.* Tunneling magnetoresistance of magnetic tunnel junctions using perpendicular magnetization L1₀-CoPt electrodes. *Appl. Phys. Lett.* **92**, 172502 (2008).
10. Yakushiji, K. *et al.* Ultrathin Co/Pt and Co/Pd superlattice films for MgO-based perpendicular magnetic tunnel junctions. *Appl. Phys. Lett.* **97**, 232508 (2010).
11. Carvello, B. *et al.* Sizable room-temperature magnetoresistance in cobalt based magnetic tunnel junctions with out-of-plane anisotropy. *Appl. Phys. Lett.* **92**, 102508 (2008).
12. Wang, W. G. *et al.* Electric-field-assisted switching in magnetic tunnel junctions. *Nat. Mater.* **11**, 64–68 (2012).
13. Wang, W. G. *et al.* Rapid thermal annealing study of magnetoresistance and perpendicular anisotropy in magnetic tunnel junctions based on MgO and CoFeB. *Appl. Phys. Lett.* **99**, 102502 (2011).
14. Meng, H. *et al.* Annealing temperature window for tunneling magnetoresistance and spin torque switching in CoFeB/MgO/CoFeB perpendicular magnetic tunnel junctions. *J. Appl. Phys.* **110**, 103915 (2011).
15. Gan, H. D. *et al.* Origin of the collapse of tunnel magnetoresistance at high annealing temperature in CoFeB/MgO perpendicular magnetic tunnel junctions. *Appl. Phys. Lett.* **99**, 252507 (2011).
16. Miyakawa, N., Worledge, D. C. & Kita, K. Impact of Ta Diffusion on the Perpendicular Magnetic Anisotropy of Ta/CoFeB/MgO. *IEEE Magn. Lett.* **4**, 1000104 (2013).
17. Parkin, S. S. P. *et al.* Giant tunnelling magnetoresistance at room temperature with MgO (100) tunnel barriers. *Nature Mater.* **3**, 862–867 (2004).
18. Suemitsu, K. *et al.* Improvement of Thermal Stability of Magnetoresistive Random Access Memory Device with SiN Protective Film Deposited by High-Density Plasma Chemical Vapor Deposition. *Jpn. J. Appl. Phys.* **47**, 2714 (2008).
19. Liu, T., Cai, J. W. & Sun, L. Large enhanced perpendicular magnetic anisotropy in CoFeB/MgO system with the typical Ta buffer replaced by an Hf layer. *AIP Advances* **2**, 032151 (2012).
20. Yang, H. X. *et al.* First-principles investigation of the very large perpendicular magnetic anisotropy at Fe/MgO and Co/MgO interfaces. *Phys. Rev. B* **84**, 054401 (2011).
21. Worledge, D. C. *et al.* Spin torque switching of perpendicular Ta/CoFeB/MgO-based magnetic tunnel junctions. *Appl. Phys. Lett.* **98**, 022501 (2011).



22. Shiota, Y. *et al.* Opposite signs of voltage-induced perpendicular magnetic anisotropy change in CoFeB/MgO junctions with different underlayers. *Appl. Phys. Lett.* **103**, 082410 (2013).
23. Alzate, J. G. *et al.* Temperature dependence of the voltage-controlled perpendicular anisotropy in nanoscale MgO/CoFeB/Ta magnetic tunnel junctions. *Appl. Phys. Lett.* **104**, 112410 (2014).
24. Hindmarch, A. T. *et al.* Zirconium as a boron sink in crystalline CoFeB/MgO/CoFeB magnetic tunnel junctions. *Appl. Phys. Express* **4**, 013002 (2011).
25. Pai, C. F. *et al.* Enhancement of perpendicular magnetic anisotropy and transmission of spin-Hall-effect-induced spin currents by a Hf spacer layer in W/Hf/CoFeB/MgO layer structures. *Appl. Phys. Lett.* **104**, 082407 (2014).
26. Niessen, A. K. & Deboer, F. R. The enthalpy of formation of solid borides, carbides, nitrides, silicides and phosphides of transition and noble metals. *J. Less-Common Met.* **82**, 75 (1981).
27. Yamanouchi, M. *et al.* Dependence of magnetic anisotropy on MgO thickness and buffer layer in Co₂₀Fe₆₀B₂₀-MgO structure. *J. Appl. Phys.* **109**, 07C712 (2011).
28. Moghadam, N. Y. & Stocks, G. M. Magnetic structure of Ni-rich Ni_{1-x}Ta_x and permalloy-Ta alloys. *Phys. Rev. B* **71**, 134421 (2005).
29. Kowalewski, M. *et al.* The effect of Ta on the magnetic thickness of permalloy (Ni₈₁Fe₁₉) films. *J. Appl. Phys.* **87**, 5732 (2000).
30. Ikeda, S. *et al.* Tunnel magnetoresistance of 604% at 300 K by suppression of Ta diffusion in CoFeB/MgO/CoFeB pseudo-spin-valves annealed at high temperature. *Appl. Phys. Lett.* **93**, 082508 (2008).
31. Lide, D. R. *CRC Handbook of Chemistry and Physics* 81st, Sec.5 (CRC, Boca Raton, FL, 2000).

Acknowledgments

This work was supported by the National Key Basic Research Program of China under Grant No. 2014CB921002, and the National Natural Science Foundation of China under Grant Nos.51171205 and 11374349. We are grateful to Professors M.J. Kramer and M.B. Sauer for their improving the manuscript English.

Author contributions

J.W.C. planned and supervised the study. T.L., Y.Z. and J.W.C. wrote the manuscript. T.L. prepared samples and carried out the magnetic property measurement. T.L., Y.Z. and H.Y.P. performed the TEM measurement. All authors analyzed the data, discussed the result and commented on the manuscript.

Additional information

Competing financial interests: The authors declare no competing financial interests.

How to cite this article: Liu, T., Zhang, Y., Cai, J.W. & Pan, H.Y. Thermally robust Mo/CoFeB/MgO trilayers with strong perpendicular magnetic anisotropy. *Sci. Rep.* **4**, 5895; DOI:10.1038/srep05895 (2014).



This work is licensed under a Creative Commons Attribution-NonCommercial-NoDerivs 4.0 International License. The images or other third party material in this article are included in the article's Creative Commons license, unless indicated otherwise in the credit line; if the material is not included under the Creative Commons license, users will need to obtain permission from the license holder in order to reproduce the material. To view a copy of this license, visit <http://creativecommons.org/licenses/by-nc-nd/4.0/>